VER
Vascular & Endovascular Review

Design, Optimization And In-Vitro–Ex-Vivo Evaluation Of Enteric-Coated Nanocarriers For Enhanced Oral Bioavailability Of A Poorly Soluble Drug

Dr. Subhranshu Panda[1], Shubham Tikait[2]*, Dr. Swati Deshmukh[3]

[1]Director, School of Pharmaceutical Sciences, Jaipur National University (JNU), Jaipur, Rajasthan-302017
[2]*Research Scholar, Jaipur National University (JNU), Jaipur, Rajasthan-302017
[3]Principal, Shraddha Institute of pharmacy (SIOPs), Washim, Maharashtra-444505

Corresponding Author,
Shubham Tikait,
Research Scholar, Jaipur National University, Jaipur, Rajasthan-302017
Email: shubhamtikait004@gmail.com

ABSTRACT

The present study aimed to design, optimize, and evaluate enteric-coated nanocarriers to enhance the oral bioavailability of Rifaximin, a poorly soluble and P-glycoprotein–susceptible drug. Preformulation studies, including organoleptic assessment, solubility profiling, FTIR, DSC, partition coefficient, hygroscopicity analysis, and micromeritic evaluation, confirmed the physicochemical suitability and compatibility of Rifaximin with glyceryl monostearate, Pluronic F68, and Eudragit L100. Solid lipid nanoparticles were prepared using a solvent-injection method and subsequently coated to obtain enteric-protected RFN-EC-SLNs. A Quality-by-Design–enabled Box–Behnken Design (BBD) was employed by varying lipid concentration, surfactant level, and polymer content to optimize critical quality attributes: particle size, entrapment efficiency, and drug release. Statistical modeling revealed significant effects of lipid and polymer levels on nanoparticle characteristics, and the optimized formulation (F6) achieved a particle size of 154 ± 14 nm, entrapment efficiency of 82 ± 0.9%, and drug release of 86 ± 1.2%.

In-vitro release studies demonstrated effective gastric protection at pH 1.2 and sustained intestinal release at pH 6.8, confirming the enteric functionality of Eudragit L100. Ex-vivo permeation across sheep intestinal mucosa showed enhanced permeation and reduced efflux, indicating improved trans-epithelial transport and P-gp modulation. Stability studies conducted under ICH conditions established the robustness, physicochemical stability, and retention of functional properties of the optimized formulation. Overall, the developed enteric-coated nanocarriers significantly improved the solubility, intestinal release, and permeation profile of Rifaximin, supporting their potential as an effective oral delivery platform for poorly soluble drugs.

KEYWORDS: Rifaximin; Solid Lipid Nanoparticles; Enteric Coating; Eudragit L100; Quality by Design (QbD); Box–Behnken Design (BBD); Oral Bioavailability; Ex-vivo Permeation; In-vitro Release; Poorly Soluble Drugs; Nanocarriers; P-glycoprotein Efflux; Optimization; Dynamic Light Scattering..

How to Cite: Dr. Subhranshu Panda, Shubham Tikait*, Dr. Swati Deshmukh, (2025) Design, Optimization And In-Vitro–Ex-Vivo Evaluation Of Enteric-Coated Nanocarriers For Enhanced Oral Bioavailability Of A Poorly Soluble Drug, Vascular and Endovascular Review, Vol.8, No.14s, 265-282.

INTRODUCTION

Rifaximin is a semi-synthetic, poorly water-soluble antibiotic widely used for the management of gastrointestinal infections, hepatic encephalopathy, traveler's diarrhea, and irritable bowel syndrome.[1-5] Despite its broad therapeutic utility and excellent safety profile, its clinical effectiveness is significantly limited by poor aqueous solubility and minimal systemic absorption following oral administration. The drug exhibits a Biopharmaceutics Classification System (BCS) Class IV profile characterized by low solubility and poor permeability which contributes to inadequate intestinal absorption and inconsistent therapeutic concentrations at the target site.[6-12] Moreover, Rifaximin is a known substrate of P-glycoprotein (P-gp), an efflux transporter abundantly expressed in the intestinal epithelium. This efflux activity restricts the trans-epithelial movement of the drug, further reducing its bioavailability and limiting therapeutic performance. Therefore, designing an efficient oral delivery system capable of enhancing solubility, modulating efflux, and improving intestinal permeability is essential.[13-18]

Lipid-based nanocarriers, particularly solid lipid nanoparticles (SLNs), have gained significant interest as promising drug-

delivery systems for poorly soluble drugs. SLNs offer advantages such as biocompatibility, controlled release behavior, high drug-loading efficiency, and protection of labile compounds from degradation. Their nano-sized structure enhances interfacial interaction with the intestinal mucosa, facilitating improved absorption and permeability. However, for drugs like Rifaximin that are unstable or incompletely released in acidic gastric conditions, the incorporation of enteric-coated polymers provides substantial benefits. An enteric-coated SLN system can protect the drug from early degradation in the stomach, ensure targeted release in the intestine, and support optimal absorption where therapeutic activity is required. Eudragit L100, an anionic pH-dependent polymer, is particularly suitable for such systems due to its selective solubility at intestinal pH and its ability to maintain formulation integrity under acidic conditions.[19-22]

The application of Quality by Design (QbD) principles in pharmaceutical development has further strengthened formulation optimization by introducing systematic design approaches, risk assessment strategies, and statistically driven experimentation. The Box–Behnken Design (BBD), a key response surface methodology, enables efficient evaluation of critical formulation variables, reducing development complexity while improving product quality and predictability. In the context of SLN systems, factors such as lipid concentration, surfactant level, and polymer content significantly influence critical quality attributes, including particle size, drug entrapment efficiency, and release behavior. Through QbD-driven optimization, robust and reproducible nanocarriers can be achieved.[23-29]

Given these considerations, the development of Rifaximin-loaded enteric-coated solid lipid nanoparticles (RFN-EC-SLNs) presents a promising strategy to overcome the drug's inherent limitations. Such a system not only enhances solubility and stability but also improves intestinal permeability and potentially reduces P-gp–mediated efflux, leading to better therapeutic outcomes. This research focuses on the formulation, optimization, characterization, and evaluation of RFN-EC-SLNs using a QbD framework, with the aim of improving oral bioavailability and establishing a reliable delivery platform for Rifaximin and other poorly soluble therapeutic agents.

MATERIALS AND METHODS

Materials:

Rifaximin was received as a gift sample from Cipla Pharmaceuticals Ltd., Mumbai. Glyceryl monostearate (GMS) and Eudragit L100 were procured from Loba Chemie and Evonik India Pvt. Ltd., respectively. Pluronic F68 was sourced from Sigma-Aldrich, USA. All solvents and reagents used, including ethanol, methanol, and acetone, were of analytical grade and purchased from Merck, Mumbai.

Preformulation studies:

Organoleptic Evaluation:

The organoleptic characteristics of Rifaximin were assessed visually and manually to confirm its compliance with pharmacopeial standards. The sample was observed under adequate lighting for colour, appearance, and uniformity. Odour was examined by gently wafting the sample, and taste was noted only by reference to documented descriptions, avoiding direct tasting for safety. Texture and physical form (fine powder, crystalline, amorphous) were evaluated by manual inspection and rubbing a small quantity between the fingers. All observations were recorded in triplicate.[30-31]

Fourier Transform Infrared Spectroscopy:

FTIR spectroscopy was conducted to investigate potential interactions between Rifaximin and formulation excipients. Samples of pure Rifaximin were prepared by triturating with potassium bromide (KBr) in a 1:100 ratio. The resulting pellets were scanned using an FTIR spectrophotometer (e.g., Bruker or PerkinElmer) in the range of 4000–400 cm^{-1}. [32]

Differential Scanning Calorimetry:

DSC analysis was employed to assess thermal behavior and drug-excipient compatibility. Approximately 2–5 mg of Rifaximin were weighed accurately and sealed in standard aluminum pans. The samples were heated from 30°C to 300°C at a rate of 10°C/min under a constant nitrogen purge. The thermograms were recorded using a calibrated DSC instrument (DSC 4000, PerkinElmer). [33]

Physicochemical Properties:

Solubility Studies:

The solubility of the drug was evaluated using a modified shake-flask method. Excess drug was added to 5 mL of each medium pH 1.2, 4.5, 6.8, and 7.4 and vortexed briefly before incubation in an orbital shaker at 37 ± 0.5 °C for 48 h. Samples were centrifuged (10,000 rpm, 15 min), filtered (0.22 μm), diluted, and analyzed spectrophotometrically. All assays were performed in triplicate, and solubility was expressed as mg/mL.[34]

Rifaximin solubility study in different lipids:

Using this technique, solid lipids (compritol® 888 ATO, stearic acid, glyceryl monostearate, and Gelucire 44/14) were placed

in several beakers and melted at a temperature higher than the lipid melting point of 50 ºC. A magnetic stirrer (Remi, Mumbai) was used to stir the lipid melt after a specified dosage of the medication (5 mg) was introduced. A centrifuge was then used to separate the organic phase from the aqueous phase. After dissolving the resultant solution in methanol, Whatman filter paper was used to filter it. The UV spectrophotometric technique was used to determine the drug content at 296 nm wavelength (UV Shimadzu 1900, Japan).[35]

Partition Coefficient (Log P / Log D):
Lipophilicity was determined using the n-octanol/water shake-flask method. Equal volumes of pre-saturated phases were mixed with known drug quantities and shaken at 25 ± 1 °C for 24 h. After phase separation, the aqueous fraction was quantified spectrophotometrically; octanol concentration was calculated by mass balance. Log P was derived from the octanol/water concentration ratio, while Log D was measured at pH 1.2, 4.5, 6.8, and 7.4 to capture ionization-dependent lipophilicity. Experiments were carried out in triplicate.[36]

Hygroscopicity & Moisture Content (Karl Fischer LOD):
Freeze-dried nanoparticles were exposed to 75% RH for 72 h to assess hygroscopicity. Moisture uptake was measured gravimetrically. Residual water content was determined using Karl Fischer coulometric titration by analyzing 20–30 mg of sample. All measurements were done in triplicate.[37-38]

Powder Flow Properties:
Flow properties were assessed to determine suitability for downstream processing. The angle of repose was measured using the funnel method. Bulk and tapped densities were obtained to calculate the compressibility index and Hausner ratio. All measurements were performed in triplicate.[39-40]

Risk assessment for Rifaximin-loaded enteric coated solid lipid nanoparticle (RFN-EC-SLN) formulation:
Risk factors were evaluated using key process parameters (CPPs) that might affect critical quality attributes (CQAs) related to RFN-EC-SLN. Using risk assessment approaches, the causal relationships between material and process parameters on the formulation's CQAs were shown. A risk estimate matrix (REM) was used to identify high-risk indications. REM (risk estimate matrix) gave high, medium, or low values to each component in order to illustrate the risk associated with certain material and process aspects of nanoformulations on their potential CQAs. The risk analysis for RFN-EC-SLN formulation in Table 1 showed that the high-risk indicators were investigated using an experimental technique. Nonetheless, the Quality Target Product Profile (QTTP), which is shown in Table 2, will be created in accordance with the main objective of the study.[40-42]

Table 1: Risk analysis for the Rifaximin-loaded enteric coated solid lipid nanoparticle formulation

CQA	Formulation risks						
	CPPs						
	Rifaximin amount	Conc. of lipid	Conc. of Ethanol	Conc. of stabilizer	Conc. of coating polymer	Sonication time	pH
Particle size (nm)	Medium	High	Low	Medium	High	Medium	Low
Entrapment efficiency (%)	High	High	Low	low	High	Medium	Medium
Drug release (%)	Medium	Medium	Low	Low	High	Low	High

CQA: *Critical Quality Attributes*, CPPs: *Critical Process Parameters.*

Table 1: Quality target product profile (QTTP) will be developed in line with the project's primary goal

Responses	Project Goals
Y_1: Particle size (nm)	Minimize
Y_2: Entrapment efficiency (%)	Maximize
Y_3: Drug release (%)	Maximize (Sustained at intestinal pH)

Rifaximin-loaded enteric-coated solid lipid nanoparticles (RFN-EC-SLN) preparation:
RFN-EC-SLN formulation was prepared by using the solvent injection technique. An appropriate amount of glyceryl

monostearate (lipid/organic phase) was dissolved in 5 mL of ethanol and melted in a water bath (Tempo Equipment Pvt. Ltd., India). The drug (20 mg) was dissolved in a lipid phase and then sonicated for 1 minute using a probe Sonicator (Qsonica Q500, Newtown, CT, USA). The aqueous phase (10 mL) containing an appropriate quantity of surfactant (Pluronic F68) was homogenized (PT 1600E, Polytron, Switzerland) at 3000 rpm for 1 hour, after the organic phase (Lipid solution) was introduced into it. In order to obtain aggregates, the mixture was ultracentrifuged (REMI laboratory Instrument, India) for 30 minutes at 10,000 rpm. These aggregates were then dispersed in 10 mL of an aqueous phase that contained a specific amount of stabilizer (polyvinyl alcohol), and the mixture was stirred for 3 hours at 1000 rpm to obtain precipitate. Further, the precipitate was added and agitated at 1000 rpm for 2 hours in 10 mL of Eudragit L100 buffer solution (6.8 pH phosphate buffer). The mixture was then sonicated for 10 minutes using a probe Sonicator to achieve the final suspension. For 30 minutes, the final suspension was centrifuged at 10,000 rpm. It was freeze-dried after coating RFN-SLN with Eudragit (Ilshin Laboratory Co Ltd, Korea).

Design of experiments and optimization of **Rifaximin-loaded enteric-coated solid lipid nanoparticles (RFN-EC-SLN)** by QbD-enabled BBD Technique:

Rifaximin-loaded enteric-coated solid lipid nanoparticles (RFN-EC-SLN) formulations were optimized using a QbD-enabled Box-Behnken statistical design (BBD) approach utilizing Design Expert (Ver. 13.0; Stat-Ease., MN, USA) software. Independent variables were distributed into three levels (-1, 0, +1): low, medium, and high levels using the BBD, a response surface approach. Responses such as Y_1: particle size, Y_2: entrapment efficiency percent (EE (%)), and Y_3: RFN release (%) were chosen as dependent factors, whereas A: the quantity of lipid, B: surfactant concentration, and C: the amount of polymer were chosen as independent variables. The response surface approach may be used to forecast how each element will interact and affect dependent variables (reactions). Eq. 1 shows a quadratic model formula for the BBD quadratic model.[43-46]

$$Y= a_0 + a_1A + a_2B + a_3C + a_{12}AB + a_{13}AC + a_{23}BC + a_{11}A^2 + a_{22}B^2 + a_{33}C^2 \ldots \textit{(Eq. 1).}$$

Where Y showed the responses, the intercept was described by a_0, the regression coefficients were depicted by a_1 to a_{33}, and the formulation attributes were expressed by A, B, and C for the Quadratic model.

Characterization RFN-EC-SLN formulation:

Particle Size, PDI, and Zeta Potential Analysis:

The mean particle size, dispersity index (PDI), and surface charge of the RFN-EC-SLN formulation were assessed using dynamic light scattering (Zetasizer Nano ZS, Malvern, UK). The PDI value was used to indicate the uniformity of particle distribution, whereas the zeta potential reflected the electrostatic stability and likelihood of particle aggregation.[47]

Entrapment Efficiency and Drug Content:

The encapsulation efficiency was determined by centrifuging 1 mL of RFN-EC-SLN dispersion (equivalent to 1 mg/mL drug) at 15,000×g for 30 min at 4 °C. The supernatant was diluted with methanol, and the unencapsulated drug was quantified spectrophotometrically at 296 nm. Entrapment efficiency (%) and drug loading (%) were calculated based on the initial and free drug concentrations.[48]

***In-Vitro* Drug Release Study:**

Drug release from the optimized enteric-coated SLN formulation was evaluated using dialysis cassettes (2,000 Da MWCO). The formulation was placed in hydrated cassettes and exposed to simulated gastric fluid (pH 1.2) for 2 h, followed by simulated intestinal fluid (pH 6.8) for 22 h under continuous stirring. Samples withdrawn at scheduled intervals were analyzed using UV-visible spectrophotometry to obtain the cumulative drug release profile.[49]

***Ex-vivo* permeation study:**

The Franz diffusion cell was used to accomplish the *ex-vivo* permeation of RFN from RFN-EC-SLN. From the nearby butcher, freshly isolated sheep intestinal mucosa was acquired. Throughout the research period, the intestinal mucosa of sheep must remain viable. Thus, after scarifying the animal, the intestinal mucosa was immediately submerged in the phosphate buffer solution (pH 6.8). The diffusion cell's standard surface area was 3.14 cm^2, and the mucosa's thickness was 0.2 cm. The donor (apical) and receptor (basolateral) compartments supported the diffusion cell on which the mucosa (3.14 cm^2) was placed. Phosphate buffer (PH 6.8) was used to adjust the volume of a cell (15 mL), and the mucosa was stabilized in the buffer for 15 minutes. A magnetic stirrer was used to continually agitate the phosphate buffer of the receptor compartment while RFN-EC-SLN formulations (1 mL equivalent to 100 µg/mL of RFN) were evenly placed in the donor compartment (apical membrane). RFN's penetration into the intestinal mucosa of sheep was measured over a period of 1–24 hours. Aliquots (0.1 mL) were taken from receptor compartments at predefined intervals (i.e., 1, 2, 4, 8, 12, and 24 hours). The fresh phosphate buffer was added at the same temperature to keep a cell's volume constant. After being diluted with methanol, the samples were centrifuged for 10 minutes at 5000 rpm. Using a validated UV-visible spectrophotometric approach, the quantity of RFN that infiltrated the sheep intestinal mucosa 24 hours after the supernatant was removed and the proper dilutions were prepared.[50]

Further, RFN is a crucial substrate of P-gp-mediated efflux, which causes substantial drug loss due to epithelial barrier

processes. The efflux ratio of the RFN-EC-SLN formulation was assessed to show the created nanosystem's anti-efflux capabilities. In order to assess the basolateral (receptor) to apical (donor) transit of RFN, a parallel experiment was carried out in the same sheep intestine mucosal system that contains Franz diffusion cells. After 24 hours, 100 µL of samples were taken once from the apical chamber (just at the terminal time point). The approved UV technique measured the quantity of RFN transferred from B to A. P_{app} (B-A) was then used to calculate the efflux ratio, as described in **Eq. 2**.

$$\text{Efflux ratio} = \frac{\text{Papp of B} - \text{A}}{\text{Papp of A} - \text{B}} \quad \ldots\ldots\ldots\ldots\ldots (\boldsymbol{Eq.2})$$

B-A is basolateral to apical; A-B is apical to basolateral, and P_{app} is the apparent permeability coefficient.

Stability Studies:

Formulation stability was assessed following ICH Q1A(R2) guidelines in a controlled chamber set at 40 ± 2 °C and 75 ± 5% RH for three months. Samples were periodically inspected for changes in particle size, PDI, zeta potential, drug content, and physical characteristics to confirm long-term formulation robustness.[51-55]

Statistical Analysis:

Utilizing GraphPad Prism 10.0, the statistical analysis was completed. *In-vitro* and *ex-vivo* experiments had n = 6 per trial and each experiment included at least three trials. The findings were reported as mean ± SD. Students' t-tests were used to estimate experimental results by contrasting unpaired samples from two groups. According to the results of the release and permeation investigations, Tukey's post hoc comparison with ANOVA and p-value were statistically significant (*p<0.05, **p<0.01, ***p<0.0005, and ****p<0.0001).[56-59]

RESULT AND DISCUSSION:

Preformulation studies:

Organoleptic Evaluation:

Rifaximin appeared as an orange-red, fine, crystalline powder with smooth texture and no detectable odour, consistent with reported pharmacopeial descriptions. The particle uniformity and free-flowing nature indicate good handling properties for formulation development.

Table 3: Organoleptic Properties of the Rifaximin

Parameter	Observation
Colour	Orange–red powder
Appearance	Fine, crystalline, free-flowing
Odour	Odourless
Taste	Not evaluated (based on literature: bitter)
Texture	Smooth, non-gritty powder

Fourier Transform Infrared Spectroscopy (FTIR):

The FTIR spectrum of the physical mixture containing Rifaximin and the selected excipients (GMS, Pluronic F68, and Eudragit L100) displayed all major characteristic peaks of each component without significant peak shifting or disappearance. Key absorption bands such as O–H/N–H stretching (3437 cm^{-1}), aliphatic C–H stretching (2925 and 2854 cm^{-1}), ester carbonyl stretching (1736 cm^{-1}), aromatic/amide vibrations (1618 and 1581 cm^{-1}), and C–O–C/C–O functional groups (1278–1080 cm^{-1}) were clearly observed.

The preservation of these peaks indicates the absence of strong chemical interactions between Rifaximin and the excipients. Thus, the components are considered compatible and suitable for nanoparticle formulation.

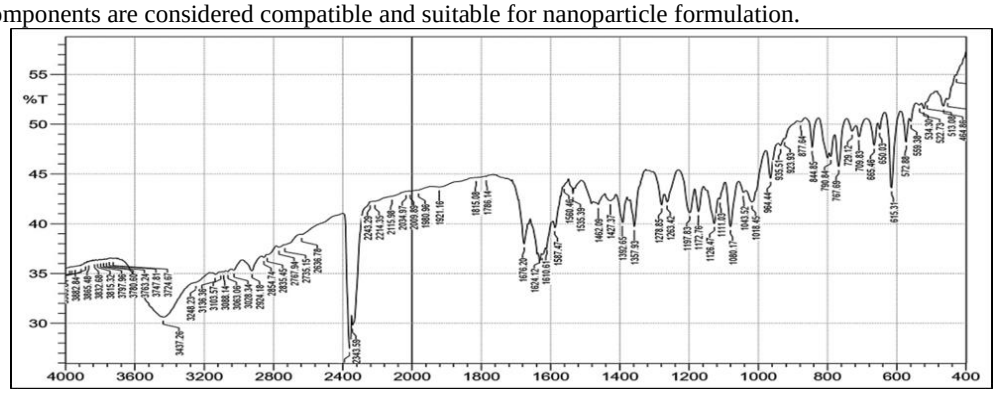

Fig. 1: FTIR Spectra of Physical mixture (Rifaximin with Glyceryl Monostearate (lipid), Pluronic F68 (surfactant), and Eudragit L100 (polymer)

Differential Scanning Calorimetry (DSC):

The DSC thermogram of the physical mixture displayed two main endothermic events. The first peak at **57.80°C** corresponds to the melting of glyceryl monostearate, while the second peak at **164.27°C** represents the thermal transition of Rifaximin, influenced slightly by the presence of Eudragit L100.

No additional or unexpected peaks appeared in the thermogram, confirming the absence of chemical interaction among components. The slight reduction and broadening of the drug's melting point suggest partial amorphization or dispersion within the excipients. Overall, the mixture shows good thermal compatibility for nanoparticle formulation.

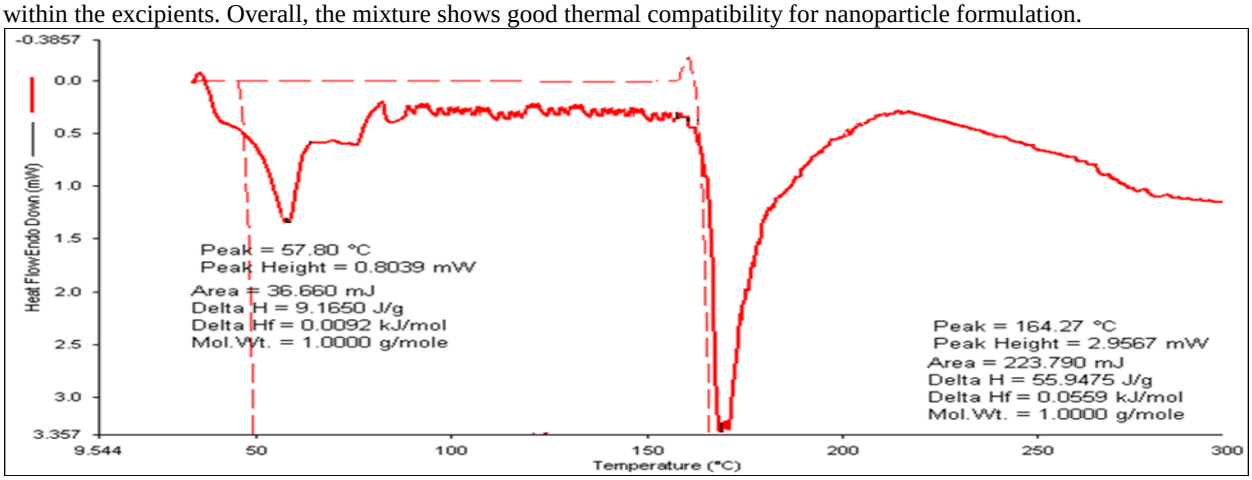

Fig. 2: DSC Thermogram of Physical mixture (Rifaximin with Glyceryl Monostearate (lipid), Pluronic F68 (surfactant), and Eudragit L100 (polymer)

Solubility Studies in different media:

The drug showed minimal solubility under acidic conditions, with solubility increasing progressively toward neutral pH, confirming a pH-dependent dissolution pattern. Surfactants, particularly Tween 80, substantially enhanced solubility through micellar solubilization. Lipid systems provided the greatest solubilization capacity, with Compritol® 888 showing the highest affinity, supporting its selection for SLN formulation due to strong drug–lipid compatibility.

Table 4: Solubility Profile of Drug

Medium / Carrier	Solubility (mg/mL) ± SD
pH 1.2	0.42 ± 0.03
pH 4.5	0.65 ± 0.02
pH 6.8	1.12 ± 0.05
pH 7.4	1.35 ± 0.04

Selection of components for formulation:

The maximum solubilizing potential of RFN was found in less glyceryl monostearate (280 mg/10 mg of RFN) and was selected as a solid lipid. Simultaneously, the highest compatibility of RFN was found with pluronic F68; therefore, it was selected as a surfactant. Eudragit L100 is an enteric-coated polymer significantly dissolved at pH >6. Therefore, it is commonly used in enteric-coated systems. Finally, all selected components' highest solubilizing and compatible potentials made them ideal for the current formulation. All selected components are biodegradable and biocompatible systems (that come under GRAS (Generally recognized as safe ingredients) for RFN-EC-SLN formulation.

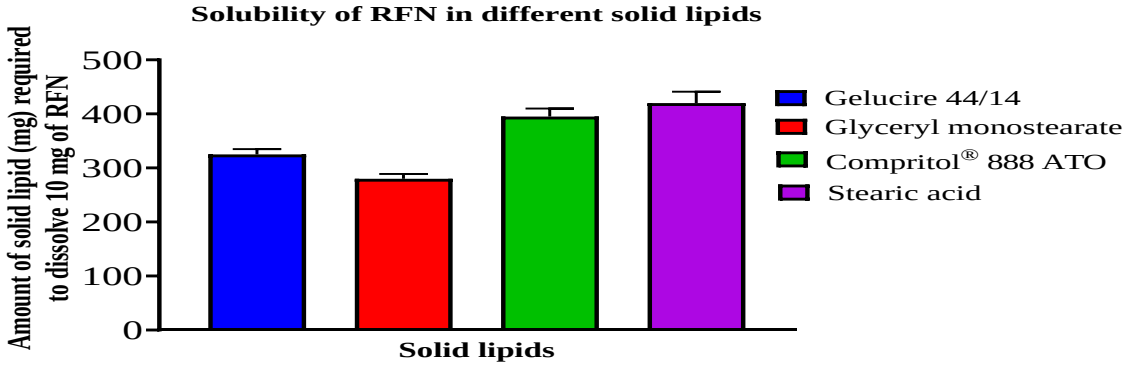

Fig. 3: Characterization of saturation solubility of RFN in different solid lipids.

Partition Coefficient (Log P / Log D):
The drug demonstrated strong affinity for the lipophilic phase (Log P > 3), confirming suitability for lipid-based systems. Log D increased with pH, indicating reduced ionization and improved lipid solubility at intestinal pH, supporting efficient entrapment in SLNs and improved absorption in higher pH regions.

Table 5: Log P and Log D Values

Parameter	pH 1.2	pH 4.5	pH 6.8	pH 7.4	Interpretation
Log P	3.12 ± 0.04	—	—	—	High intrinsic lipophilicity
Log D	2.46 ± 0.03	2.83 ± 0.05	3.01 ± 0.04	3.05 ± 0.06	Higher Log D at neutral pH supports lipid-based delivery

Hygroscopicity & Moisture Content (Karl Fischer LOD):
The freeze-dried nanoparticles showed low moisture uptake and minimal residual water, confirming a stable, non-hygroscopic powder suitable for long-term storage and preventing aggregation or hydrolysis.

Table 6: Hygroscopicity & Moisture Content

Parameter	Value (Mean ± SD)	Interpretation
Moisture Uptake at 75% RH	1.82 ± 0.07%	Low hygroscopicity
Karl Fischer Moisture Content	1.25 ± 0.04%	Efficient lyophilization and good stability

Powder Flow Properties:
The freeze-dried powder exhibited good flowability with acceptable compressibility and low cohesion, indicating suitability for handling and solid-dosage manufacturing processes.

Table 7: Micromeritic Properties of Freeze-Dried Nanoparticles

Parameter	Value (Mean ± SD)
Angle of Repose (°)	32.4 ± 0.88
Bulk Density (g/mL)	0.29 ± 0.01
Tapped Density (g/mL)	0.36 ± 0.01
Compressibility Index (%)	19.44 ± 0.62
Hausner Ratio	1.24 ± 0.02

Design of experiments and optimization RFN-EC-SLN by QbD-enabled BBD Technique:
Thirteen formulations of Rifaximin-loaded enteric-coated solid lipid nanoparticles (RFN-EC-SLN) (F1–F13; Table 8) were prepared using the solvent injection method. These formulations were optimized using a Quality by Design (QbD) approach integrated with the Design of Experiments (DOE). This optimization process helped determine how formulation variables, including A (lipid phase concentration), B (surfactant concentration), and C (enteric polymer concentration), influenced critical responses: Y_1 (particle size), Y_2 (entrapment efficiency, EE%), and Y_3 (drug release %). The intended Quality Target Product Profile (QTTP) and rationale for optimizing the RFN-EC-SLN system are outlined. For the development of these nanoparticles, the lipid phase was varied between 50–150 mg, the surfactant between 200–600 mg, and the enteric-coated polymer between 40–80 mg. Additionally, the actual values closely matched the predicted ones for every response. The statistical impacts of the lipid/organic phase, surfactant, and Eudragit L100 interaction on Y_1, Y_2, and Y_3. For the quadratic model, specific component concentrations were significant, yielding p-values of 0.0391, 0.0316, and 0.0441 for Y_1, Y_2, and Y_3, respectively. Therefore, Y_1-Y_3 are significantly impacted (*$p < 0.05$) by the interplay of variables A and C (alterations in the quantities of glyceryl monostearate and Eudragit L100). At the same time, factor B (surfactant) had little impact on the response. Based on these findings, the quadratic model was employed to evaluate the design space for optimization. The polynomial equations generated for the interaction of formulation variables with responses (Eqs. 3-5) demonstrated that factor A had the most substantial coefficient values for Y_1 (+205 nm), Y_2 (+73%), and Y_3 (+78%), underscoring the strong impact of lipid phase concentration on the system's characteristics.

Particle size (Y_1) = $+205.00+64.12*A-22.75*B+13.13*C-15.75*AB+4.00*AC-2.75*BC$
$+47.00*A^2-16.25*B^2-9.50*C^2$ … **(Eq. 3).**

EE (%) (Y_2) = $+73.00+3.12*A+3.37*B+1.75*C+1.00*AB-1.75*AC-0.7500*BC-2.75*A^2$
$+2.25*B^2+3.50*C^2$ … **(Eq. 4).**

Drug release (%) (Y_3) = $+78.00-4.13*A+2.62*B-5.00*C-1.75*AB+0.5000*AC+0.5000*BC$
$-1.12*A^2-0.6250*B^2+0.6250*C^2$ … **(Eq. 5).**

The results from these equations were consistent with the 3D response surface plots presented in Figs. 4 A–C shows that increased amounts of glyceryl monostearate and Eudragit L100 resulted in larger particle sizes and higher entrapment efficiency while decreasing drug release percentages. Lipid concentration increased as a result, perhaps increasing the size and EE (%) of the RFN-EC-SLN system. Larger particles, on the other hand, can restrict drug penetration and absorption, leading to drug breakdown and elimination in the GIT. The % error, which was less than 5%, showed that the projected and experimental values were very close (Figs. 4D-F) indicates the precision of the model in predicting formulation findings. However, Figs. 5 A-C represented the contour plots for the effect of independent variables on responses. The findings of contour plots demonstrated the quadratic model because the lines from contour plots showed a curvy shape. This indicates that the developed design is relevant to the quadratic model. These minimum errors demonstrated the reliability of generated equations for forecasting the formulation's behavior. Batch F6 was an optimized formulation using 20 mg Rifaximin, 100 mg glyceryl monostearate, 600 mg Pluronic F68, and 40 mg Eudragit L100. The finalized optimized composition is detailed in Table 9**.** This formulation achieved desirable parameters: entrapment efficiency of 82 ± 0.9%, particle size of 154 ± 14 nm, and drug release of 86 ± 1.2%. Due to these results aligning precisely with the predicted outcomes, this optimized RFN-EC-SLN formulation (F6) was selected for further characterization studies.

After analysis, the signal-to-noise ratios were 9.60, 11.08, and 9.54 for all Y_1, Y_2, and Y_3, respectively. Therefore, it indicates an adequate signal and quadratic model suitable for navigating the design space, further supporting the results. However, the model F-value of 10.52, 12.26, and 9.65 implies that the model is significant. There is only a 3.91, 3.16, and 4.41% probability that an F-value this large could be obtained due to noise. All results have supported that the current design is highly suited to the quadratic model, and the optimized formulation is fitted with all predicted limits of their responses.

Table 8: Optimization of Rifaximin-loaded enteric-coated solid lipid nanoparticles (RFN-EC-SLN) formulation.

Formulation	Drug	Formulation factors			Responses		
		Conc. of Lipid (mg)	Conc. of Surfactant (mg)	Conc. polymer (mg)	Particle size (nm)	Entrapment efficiency (%)	Drug release (%)
F1	20	50	600	60	152	72	84
F2	20	50	200	60	192	67	75
F3	20	50	400	80	182	75	78
F4	20	50	400	40	174	66	87
F5	20	100	200	40	168	74	82
F6	***20***	***100***	***600***	***40***	***154***	***82***	***86***
F7	20	100	600	80	185	82	75
F8	20	100	400	60	205	73	78
F9	20	100	200	80	210	77	69
F10	20	150	200	60	351	71	72
F11	20	150	600	60	248	80	74
F12	20	150	400	80	319	78	69
F13	20	150	400	40	295	76	76

Independent Variables	Level used, actual coded		
	Low (-1)	Medium (0)	High (+1)
A= Lipid: Glyceryl monostearate (mg)	50	100	150
B= Surfactant: Pluronic F68 (mg)	200	400	600
C= Polymer: Eudragit L100 (mg)	40	60	80

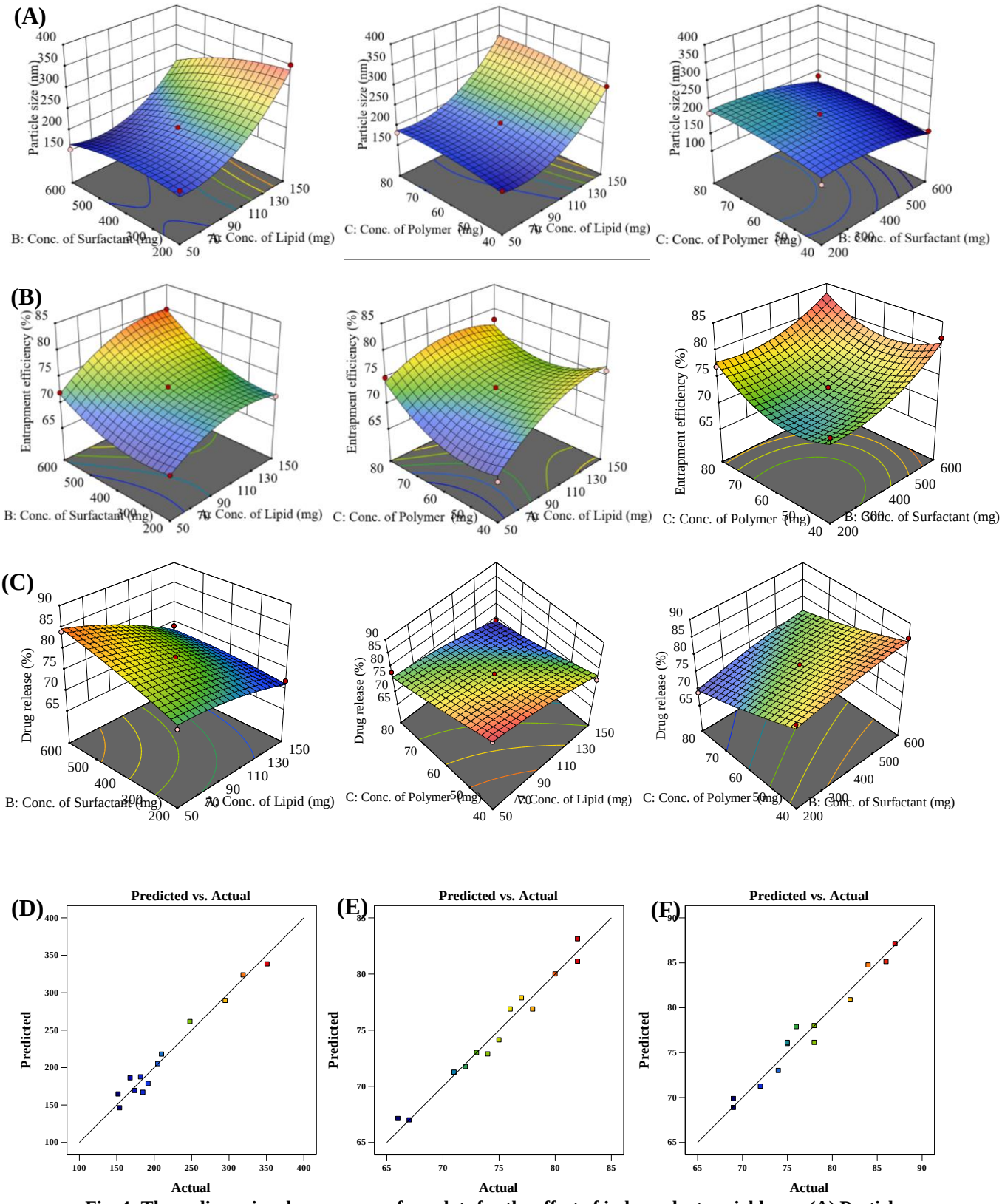

Fig. 4: Three-dimensional response surface plots for the effect of independent variables on (A) Particle size, (B) Entrapment efficiency (%), and (C) Drug release (%). Linear correlation plots between the actual and predicted values for (D) Particle size, (E) Entrapment efficiency (%), and (F) Drug release (%)

Table 9: Final composition of Rifaximin-loaded enteric-coated solid lipid nanoparticles (RFN-EC-SLN) formulation (20 mL)

Sr. No.	Category	Name	Optimized RFN-EC-SLN
1	Drug	Rifaximin	20 mg
2	**Solid lipid**	**Glyceryl monostearate**	100 mg
3	Solvent	Ethanol	5 mL
4	Surfactant	Pluronic F68	600 mg
5	Stabilizer	Polyvinyl alcohol	50 mg
6	Enteric coated polymer	Eudragit L100	40 mg
7	Solvent	Water	Up to 20 mL

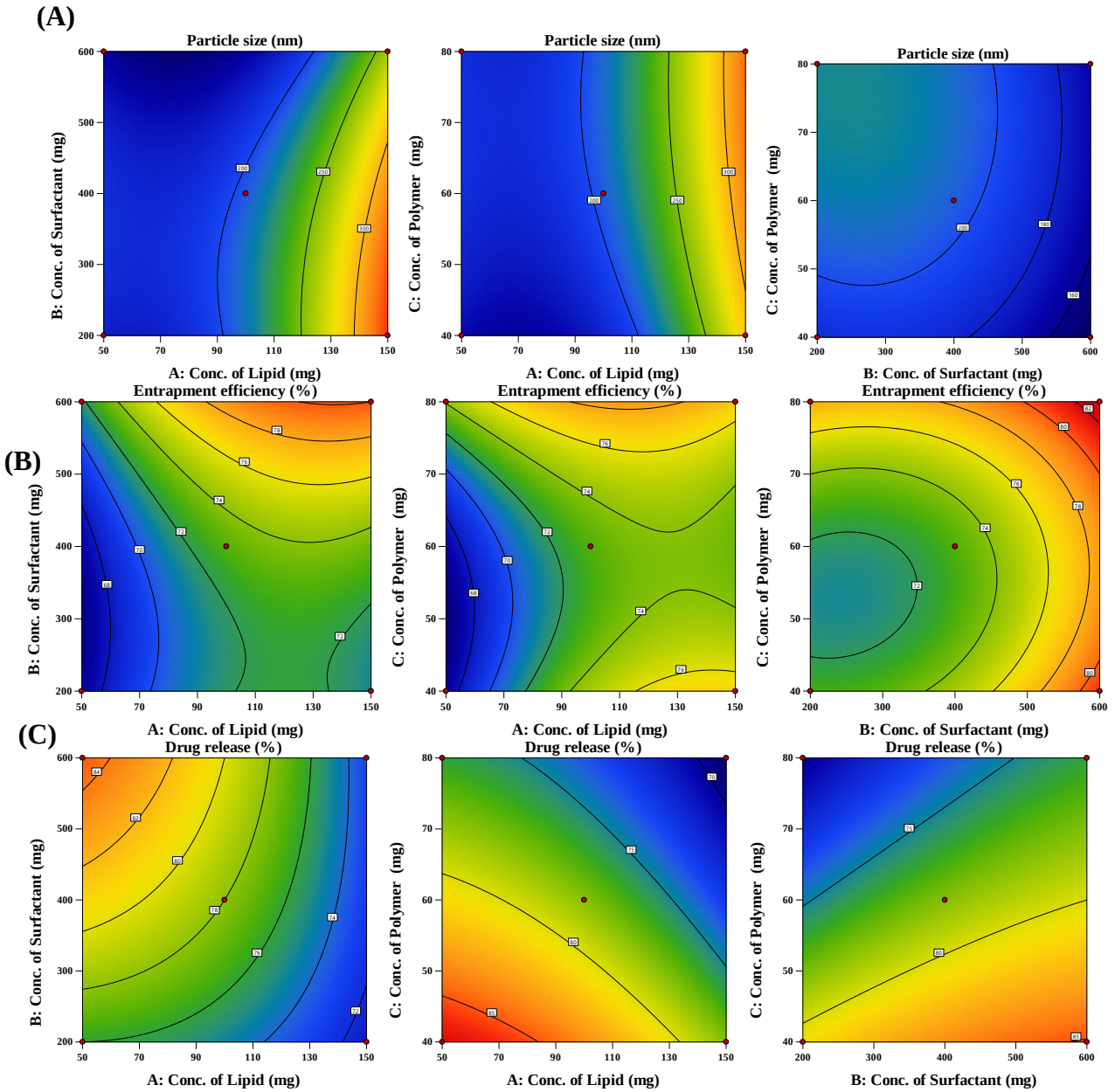

Fig. 5: Contour plots for the effect of independent variables on (A) particle size, (B) entrapment efficiency (%), and (C) drug release (%)

The adequate precision measures the signal to noise ratio and a ratio was found to be greater than 4 for all responses, which is considered as desirable. After analysis, obtained signal to noise ratio was 9.4 for all responses. Therefore, indicates an adequate signal and quadratic model highly suitable to navigate the design space. However, the **model F-value** of 9.24, 10.48 and 10.03 implies the model is significant. There is only a 3.93, 4.68 and 4.18% chance that an F-value this large could occur due to noise. All results have been supported that the current design is highly suited with quadratic model and the optimized formulation fitted with all predicted limits of their responses.

Particle size, PDI, Zeta Potential, Entrapment efficiency and drug content:
The optimized RFN-EC-SLN formulation showed a mean particle size of 154 ± 2.6 nm, confirming a nanoscale system capable of improving gastrointestinal absorption through enhanced surface area and dissolution. The PDI value of 0.21 ± 0.03 reflected a uniform and stable nanoparticle distribution. The zeta potential of +17.5 ± 0.04 mV, attributed to the cationic nature of Eudragit L100, indicated sufficient electrostatic repulsion to prevent aggregation and maintain colloidal stability. The formulation demonstrated an entrapment efficiency of 82.0 ± 1.6% and drug loading of 10.2 ± 0.2%, confirming efficient incorporation of rifaximin into the lipid matrix. These characteristics collectively support the suitability of the optimized nanoparticles for enhancing oral delivery and therapeutic performance.

***In-vitro* Drug Release Studies:**
A total of thirteen formulations were evaluated for their in-vitro drug release profiles. Among these, formulation F6 was identified as the most promising based on optimization criteria suggested by the Box–Behnken Design (BBD) and design expert analysis. The release profile of RFN from the optimized RFN-EC-SLN formulation (F6) was assessed using dialysis cassettes with a molecular weight cutoff of 2,000 Da. In simulated gastric fluid (pH 1.2), the formulation exhibited a limited release of 15.8 ± 3.4% RFN over the initial 2 hours, demonstrating gastric resistance. When transitioned to simulated intestinal fluid (pH 6.8), a sustained release pattern was observed, with cumulative RFN release reaching 86.0 ± 2.4% over 24 hours.

The release kinetics were evaluated to understand the mechanism of RFN release from the SLN matrix. Regression analysis indicated a strong correlation with the zero-order kinetic model ($R^2 = 0.989$), suggesting that the release was concentration-independent and primarily governed by a diffusion-controlled mechanism. Compared to a standard RFN suspension, the SLN formulation exhibited significantly sustained and controlled drug release over the 24-hour period ($^*p < 0.05$), confirming its potential for prolonged therapeutic action.

Table 10: *In-vitro* release of RFN from all developed formulations for 24 hours.

Sr. No.	Formulation code	RFN release after 24 hours	Amount of RFN (µg/mL) release from RFN-EC-SLN after 24 hours
1	F1	84 ± 1.2	420
2	F2	75 ± 1.4	375
3	F3	78 ± 1.6	390
4	F4	87 ± 0.6	435
5	F5	82 ± 1.9	410
6	***F6***	***86 ± 2.4***	***430***
7	F7	75 ± 2.6	375
8	F8	78 ± 2.3	390
9	F9	69 ± 0.7	345
10	F10	72 ± 1.1	360
11	F11	74 ± 1.3	370
12	F12	69 ± 0.9	345
13	F13	76 ± 1.4	380

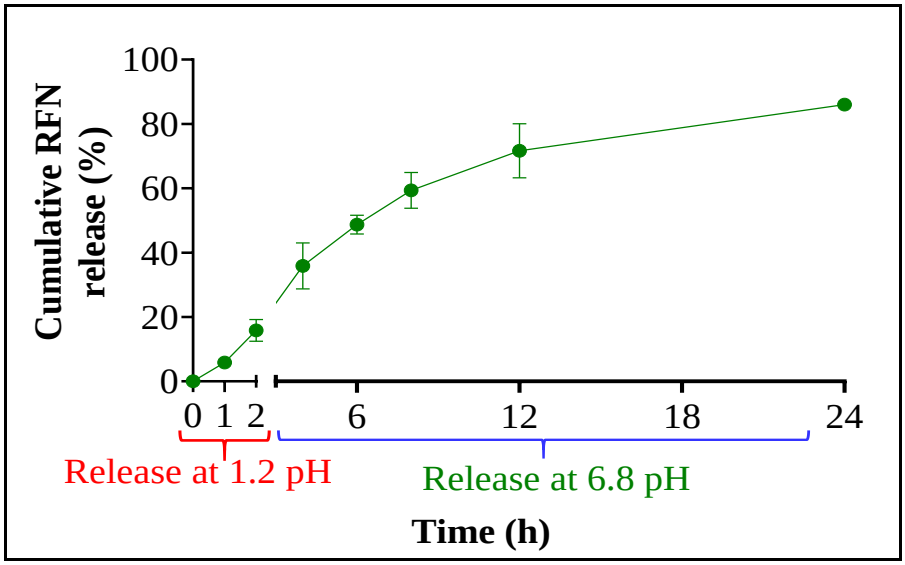

Fig. 6: Cumulative RFN release from RFN-EC-SLN over 24 hours via a dialysis cassette

Table 11: The regression coefficient of kinetic models observed for RFN-EC-SLN formulation

Release kinetic models	Formulation
	RFN-EC-SLN (R^2)
Zero-order	0.989
First-order	0.794
Higuchi	0.889
Hixon-Crowell cube root	0.988
Korsmeyer-Peppas n = Release exponent	0.916 (n = 1.801)

Data expressed as mean ± SD (*n*=3)

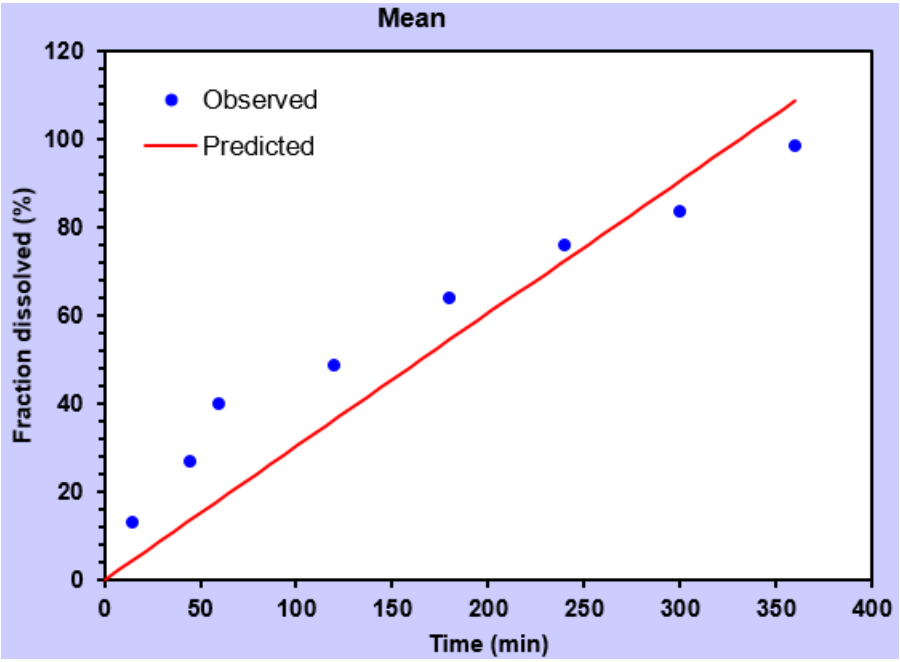

Fig. 7: Zero order profile for Formulation (F6)

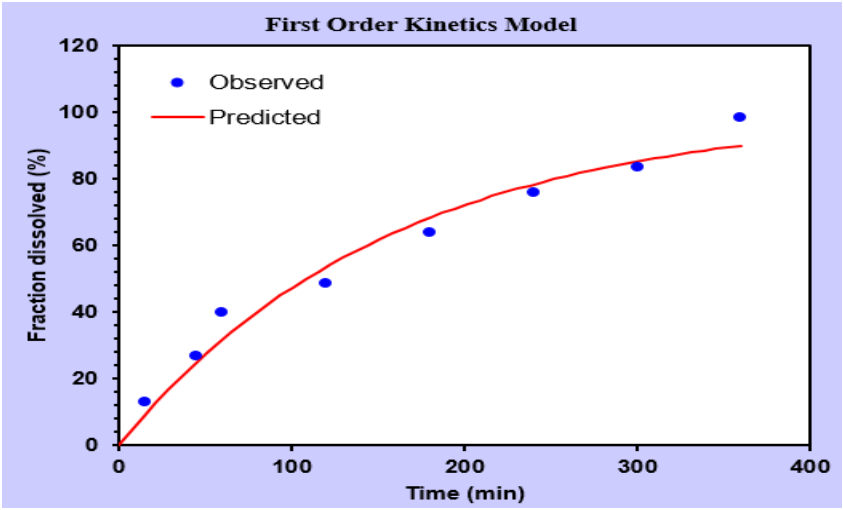

Fig. 8: First order profile for Formulation (F6)

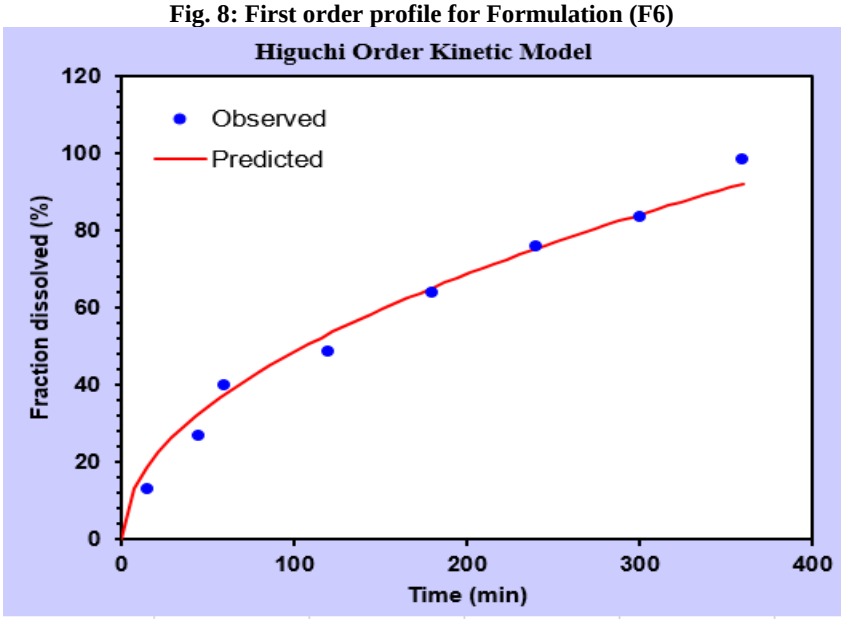

Fig. 9: Higuchi order profile for Formulation (F6)

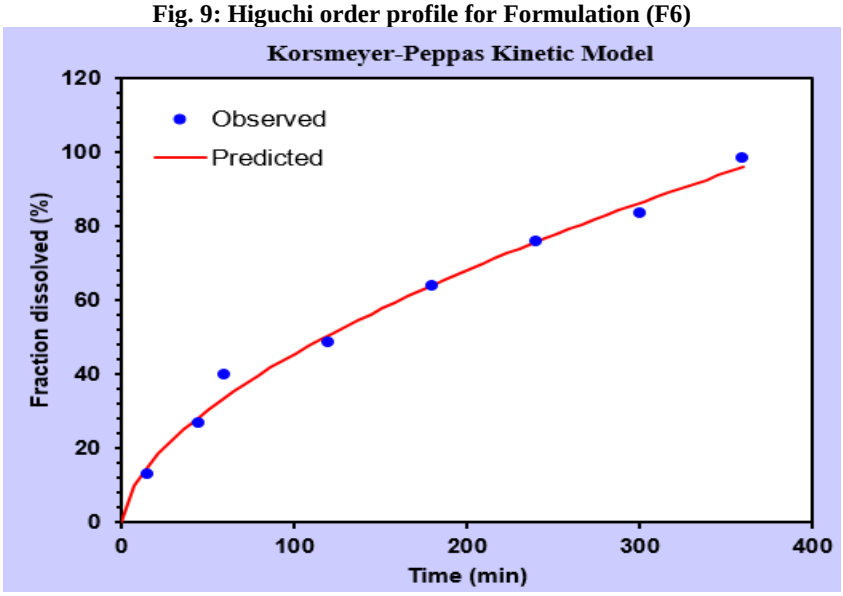

Fig. 10: Korsmeyer-Peppas order profile for Formulation (F6)

***Ex-vivo* permeation study:**

The permeability of RFN-EC-SLN was investigated using sheep intestinal mucosa employing Frans diffusion cells to assess drug transport and possible efflux inhibition. The proposed formulation was permeabilized across the intestinal mucosa of sheep using a pH 6.8 phosphate buffer medium. The results of the permeation study after RFN-EC-SLN treatment showed markedly improved drug transport across the mucosa, with 96.4 ± 9.7 µg of RFN permeation after 24 hours, as opposed to 49.8 ± 1.6 µg from the standard RFN solution at the same concentration (100 µg/mL) (Fig.11A). The enhanced surface area and formulation stability of the SLN, which both encourage quicker and more effective permeation, are responsible for this improvement.

Furthermore, RFN-EC-SLN enhanced the steady-state flux (J_{ss}) and apparent permeability coefficient (P_{app}). The SLN obtained values of 3.4×10^{-6} cm/h and 3.4×10^{-8} µg/cm²/h, respectively, while the RFN solution had a P_{app} of 1.5×10^{-6} cm/h and a J_{ss} of 1.5×10^{-8} µg/cm²/h (Figs. 11A&B). These improvements are probably the result of the formulation's surfactants, which raise membrane permeability and momentarily loosen tight junctions.

The efflux behavior of RFN was also examined using a Franz diffusion cell setup since it is a recognized P-glycoprotein (P-gp) substrate. It was discovered that the RFN solution had an efflux ratio of 1.6. However, the RFN-EC-SLN formulation dropped the ratio to 0.08 (Table 12), indicating less active drug redistribution inside the corresponding lumen. According to this, RFN-EC-SLN improved drug retention at the absorption site and increased bioavailability after oral administration by avoiding P-gp efflux activity.

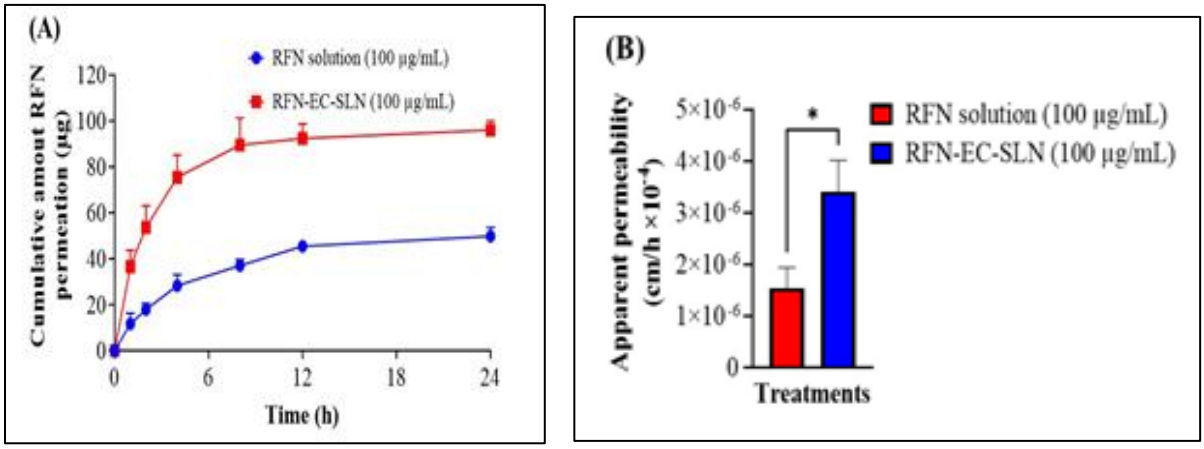

Fig. 11: (A) Cumulative RFN permeation across sheep intestinal mucosa through Franz diffusion cell after 24 hours treatment of 100 µg/mL of RFN solution and RFN-EC-SLN (B) Apparent permeability of 100 µg/mL RFN solution and RFN-EC-SLN

Table 12: P-glycoprotein efflux ratio for apical to basal and basal to apical permeation

Formulation	Papp (cm/h × 10^{-x}) (A-B)	Papp (cm/h × 10^{-x}) (B→A)	Efflux Ratio
RFN solution (100 µg/mL)	1.5×10^{-6}	2.5×10^{-6}	1.6
RFN-EC-SLN (100 µg/mL)	3.4×10^{-6}	2.9×10^{-7}	0.08

RFN: Rifaximin solution, RFN-EC-SLN: Rifaximin-loaded enteric coated solid lipid nanoparticle, P_{app}: Apparent Permeability, A→B: Apical to Basolateral, B→A: Basolateral to Apical

Table 13: Steady-state flux and cumulative RFN permeated across the intestinal mucosa

Formulation	Flux Jss (µg/cm²/h) (A→B)	Flux Jss (µg/cm²/h) (B→A)	Cumulative RFN permeated at 3 h (µg)
RFN solution (100 µg/mL)	1.5×10^{-8}	2.5×10^{-8}	49.8 ± 1.6
RFN-EC-SLN (100 µg/mL)	3.4×10^{-8}	2.9×10^{-9}	96.4 ± 9.7

RFN: Rifaximin solution, RFN-EC-SLN: Rifaximin-loaded enteric coated solid lipid nanoparticle, Jss: Steady-state flux, A→B: Apical to Basolateral, B→A: Basolateral to Apical

Stability Studies:

Accelerated stability studies were conducted for the optimized RFN-EC-SLN formulation as per ICH guidelines. Key parameters including particle size, % entrapment efficiency, PDI, zeta potential, pH, and drug loading remained within acceptable limits throughout the three-month study. No signs of instability such as phase separation or physical changes were observed. Drug content remained stable, with RFN loading at 9.95 ± 0.1% (79.6 ± 2.9%), closely matching the initial values of 10.2 ± 0.2% (82.0 ± 1.6%). These findings confirm the formulation's excellent physical and chemical stability under accelerated conditions.

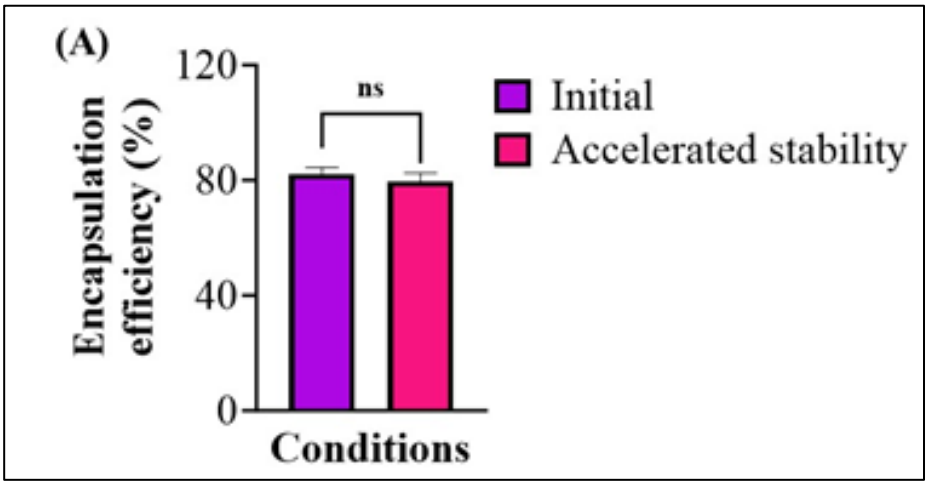

Fig. 12: (A) Encapsulation of RFN-EC-SLN at different stability conditions, i.e., initial and accelerated conditions after 3 months.

Table 14: Stability Study Data of RFN-EC-SLN

Parameters	Initial	Accelerated Stability (After 3 Months)
Particle size (nm)	154 ± 2.6	158 ± 4.2
Polydispersity index	0.21 ± 0.03	0.24 ± 0.04
Zeta potential (mV)	+17.5 ± 0.04	+17.2 ± 0.08
Phase separation	No	No
Physical appearance	Clear	Clear
pH	6.9 ± 0.2	6.8 ± 0.4
RFN content over the period (%)	10.2 ± 0.2	9.95 ± 0.1

CONCLUSION

The present study successfully demonstrated the development, optimization, and comprehensive evaluation of Rifaximin-loaded enteric-coated solid lipid nanoparticles (RFN-EC-SLNs) designed to enhance the oral bioavailability of a poorly soluble drug. Preformulation studies confirmed the physicochemical suitability of Rifaximin and compatibility with selected excipients, as supported by FTIR and DSC analyses. Solubility, partition coefficient, and lipid-screening studies validated the rationale for selecting glyceryl monostearate, Pluronic F68, and Eudragit L100 for nanoparticle fabrication.

A robust QbD-enabled Box–Behnken Design (BBD) approach established the critical influence of lipid and polymer concentrations on particle size, entrapment efficiency, and drug release. The optimized formulation (F6) achieved a desirable particle size (~154 nm), high entrapment efficiency (~82%), and sustained drug release under intestinal pH conditions, confirming the success of the optimization strategy.

In-vitro drug release studies demonstrated effective gastric protection and pH-triggered release, validating the functionality of the enteric coating. Ex-vivo permeation studies further confirmed enhanced intestinal permeation and reduced efflux, overcoming P-gp–mediated transport limitations typically associated with Rifaximin. Stability studies established that the developed formulation remained physically and chemically stable under accelerated conditions, indicating suitability for long-term storage.

Overall, the study provides strong evidence that RFN-EC-SLNs significantly improve solubility, protection, permeability, and

release characteristics of Rifaximin, highlighting their potential as an advanced oral delivery system for poorly soluble drugs.

ACKNOWLEDGMENT

The authors gratefully acknowledge the **Department of Pharmaceutical Sciences, Jaipur National University, Jaipur**, for providing the necessary facilities and support to carry out this research work successfully.

AUTHORS CONTRIBUTIONS

All authors participated equally in the preparation and development of this manuscript.

CONFLICTS OF INTERESTS

All authors have declared no conflict of interest.

REFERENCES

1. Akbarzadeh, A., Rezaei-Sadabady, R., Davaran, S., Joo, S. W., Zarghami, N., Hanifehpour, Y., Samiei, M., Kouhi, M., & Nejati-Koshki, K. (2013). Liposome: Classification, preparation, and applications. *Nanoscale Research Letters, 8*(1), 102. https://doi.org/10.1186/1556-276X-8-102
2. Alqahtani, M. S., Kazi, M., Alsenaidy, M. A., & Ahmad, M. Z. (2021). Advances in oral drug delivery. *Frontiers in Pharmacology, 12*, 618411. https://doi.org/10.3389/fphar.2021.618411
3. Arafat, M., Kirchhoefer, C., Mikov, M., Sarfraz, M., & Löbenberg, R. (2017). Nanosized liposomes containing bile salt to enhance oral bioavailability of BCS class III drug. *Journal of Pharmaceutical Sciences, 20*, 305–318. https://doi.org/10.18433/J3CK88
4. Babadi, D., Dadashzadeh, S., Osouli, M., Abbasian, Z., Daryabari, M. S., Sadrai, S., & Haeri, A. (2021). Biopharmaceutical and pharmacokinetic aspects of nanocarrier-mediated delivery of poorly soluble drugs. *Journal of Drug Delivery Science and Technology, 62*, 102324. https://doi.org/10.1016/j.jddst.2021.102324
5. Bajka, B. H., Rigby, N. M., Cross, K. L., Macierzanka, A., & Mackie, A. R. (2015). Small intestinal mucus: Influence on particle transport ex vivo. *Colloids and Surfaces B, 135*, 73–80. https://doi.org/10.1016/j.colsurfb.2015.07.038
6. Braga Emidio, N., Tran, H. N. T., Andersson, A., Dawson, P. E., Albericio, F., Vetter, I., & Muttenthaler, M. (2021). Improving gastrointestinal stability of linaclotide. *Journal of Medicinal Chemistry, 64*, 8384–8390. https://doi.org/10.1021/acs.jmedchem.1c00380
7. Cagdas, M., Sezer, A. D., & Bucak, S. (2014). Liposomes as potential drug-carrier systems. *InTechOpen*. https://doi.org/10.5772/58459
8. Danaei, M., Dehghankhold, M., Ataei, S., Hasanzadeh Davarani, F., Javanmard, R., Dokhani, A., Khorasani, S., & Mozafari, M. R. (2018). Particle size and PDI in lipid nanocarriers. *Pharmaceutics, 10*(2), 57. https://doi.org/10.3390/pharmaceutics10020057
9. Elsayad, M. K., Mowafy, H. A., Zaky, A. A., & Samy, A. M. (2021). Chitosan-caged liposomes to enhance oral bioavailability. *Pharmaceutical Development and Technology, 26*, 316–327. https://doi.org/10.1080/10837450.2020.1870237
10. Ghassemi, S., Haeri, A., Shahhosseini, S., & Dadashzadeh, S. (2018). Labrasol-enriched nanoliposomes for improved oral absorption of carvedilol. *AAPS PharmSciTech, 19*, 2961–2970. https://doi.org/10.1208/s12249-018-1118-9
11. Gouda, A., Sakr, O. S., Nasr, M., & Sammour, O. (2021). Ethanol injection technique for liposome formulation. *Journal of Drug Delivery Science and Technology, 61*, 102174. https://doi.org/10.1016/j.jddst.2020.102174
12. He, H., Lu, Y., Qi, J., Zhu, Q., Chen, Z., & Wu, W. (2019). Adapting liposomes for oral delivery. *Acta Pharmaceutica Sinica B, 9*, 36–48. https://doi.org/10.1016/j.apsb.2018.06.005
13. Homayun, B., Lin, X., & Choi, H.-J. (2019). Challenges and progress in oral delivery of biopharmaceuticals. *Pharmaceutics, 11*(3), 129. https://doi.org/10.3390/pharmaceutics11030129
14. Jaafar-Maalej, C., Diab, R., Andrieu, V., Elaissari, A., & Fessi, H. (2010). Ethanol injection method for liposomes. *Journal of Liposome Research, 20*, 228–243. https://doi.org/10.3109/08982100903347923
15. Jansook, P., & Loftsson, T. (2009). Cyclodextrins as solubilizers. *International Journal of Pharmaceutics, 379*, 32–40. https://doi.org/10.1016/j.ijpharm.2009.06.005
16. Jin, Y., Wen, J., Garg, S., Liu, D., Zhou, Y., Teng, L., & Zhang, W. (2013). Niosomes for oral delivery of Ginkgo biloba. *International Journal of Nanomedicine, 8*, 421–430. https://doi.org/10.2147/IJN.S37984
17. Kulkarni, S. B., Betageri, G. V., & Singh, M. (1995). Factors affecting microencapsulation in liposomes. *Journal of Microencapsulation, 12*, 229–246. https://doi.org/10.3109/02652049509010292
18. Large, D. E., Abdelmessih, R. G., Fink, E. A., & Auguste, D. T. (2021). Liposome composition in drug delivery. *Advanced Drug Delivery Reviews, 176*, 113851. https://doi.org/10.1016/j.addr.2021.113851
19. Lee, M. K. (2020). Liposomes for enhanced bioavailability. *Pharmaceutics, 12*, 264. https://doi.org/10.3390/pharmaceutics12030264
20. Liu, W., Ye, A., Han, F., & Han, J. (2019). Liposome digestion and GIT modeling. *Advances in Colloid and Interface Science, 263*, 52–67. https://doi.org/10.1016/j.cis.2018.11.007
21. Loftsson, T., Jarho, P., Másson, M., & Järvinen, T. (2005). Cyclodextrins in drug delivery. *Expert Opinion on Drug Delivery, 2*, 335–351. https://doi.org/10.1517/17425247.2.1.335
22. Lombardo, D., & Kiselev, M. A. (2022). Liposome preparation methods. *Pharmaceutics, 14*, 543. https://doi.org/10.3390/pharmaceutics14030543
23. Luo, Z., Paunović, N., & Leroux, J.-C. (2021). Physical methods to enhance drug absorption. *Advanced Drug Delivery Reviews, 175*, 113814. https://doi.org/10.1016/j.addr.2021.05.024

24. Nguyen, T. X., Huang, L., Gauthier, M., Yang, G., & Wang, Q. (2016). Liposome surface modification. *Nanomedicine, 11*, 1169–1185. https://doi.org/10.2217/nnm.16.9
25. Nguyen, T. X., Huang, L., Liu, L., Abdalla, A. M. E., Gauthier, M., & Yang, G. (2014). Chitosan-coated nanoliposomes for oral berberine. *Journal of Materials Chemistry B, 2*, 7149–7159. https://doi.org/10.1039/C4TB00876F
26. Panwar, P., Pandey, B., Lakhera, P. C., & Singh, K. P. (2010). Albendazole-loaded liposomes. *International Journal of Nanomedicine, 5*, 101–108. https://doi.org/10.2147/IJN.S8030
27. Schwendener, R. A., & Schott, H. (2010). Liposome formulations of hydrophobic drugs. *Methods in Molecular Biology, 605*, 129–138. https://doi.org/10.1007/978-1-60327-360-2_8
28. Torchilin, V. P. (2005). Advances in liposomes as drug carriers. *Nature Reviews Drug Discovery, 4*, 145–160. https://doi.org/10.1038/nrd1632
29. Vemuri, S., & Rhodes, C. T. (1995). Preparation and characterization of liposomes. *Pharmaceutica Acta Helvetiae, 70*, 95–111. https://doi.org/10.1016/0031-6865(95)00010-7
30. Wang, M., Liu, M., Xie, T., Zhang, B.-F., & Gao, X.-L. (2017). Chitosan-modified liposomes for oral progesterone. *Colloids and Surfaces B, 159*, 580–585. https://doi.org/10.1016/j.colsurfb.2017.08.028
31. Agnihotri SA, Mallikarjuna NN, Aminabhavi TM. Chitosan-based micro- and nanoparticles in drug delivery. J Control Release. 2004;100:5-28. doi:10.1016/j.jconrel.2004.08.010.
32. Ba B, Gaudin K, Désiré A, et al. Enhancing ceftriaxone absorption for noninvasive delivery. Antimicrob Agents Chemother. 2018;62(12). doi:10.1128/AAC.01170-18.
33. Patel V, Agrawal YK, Saraf S. Enteric-coated nanoparticles for targeted oral delivery of a poorly water-soluble drug: formulation and pharmacokinetic assessment. Drug Deliv Transl Res. 2019;9(4):789-801. doi:10.1007/s13346-019-00632-3.
34. Garg NK, Singh B, Jain A, Sharma R. Development and optimization of enteric-coated nanoparticles for enhanced oral bioavailability of a BCS Class II drug. J Nanopart Res. 2018;20:156. doi:10.1007/s11051-018-4257-8.
35. Rasve VR, Chakraborty AK, Jain SK, Vengurlekar S. Comparative evaluation of antidiabetic activity of ethanolic leaves extract of *Clematis triloba* and their SMEDDS formulation in streptozotocin-induced diabetic rats. J Popul Ther Clin Pharmacol. 2022;29(4):959-71. doi:10.53555/jptcp.v29i04.2360.
36. Yadav D, Kumar N. Formulation and characterization of enteric-coated polymeric nanoparticles for pH-sensitive delivery of a poorly soluble anticancer drug. AAPS PharmSciTech. 2017;18(6):2187-96. doi:10.1208/s12249-016-0696-7.
37. Singh A, Bajpai M. Optimization of Eudragit-based enteric nanoparticles for colon-targeted delivery of a hydrophobic drug using Box–Behnken design. Drug Dev Ind Pharm. 2016;42(8):1316-27. doi:10.3109/03639045.2015.1135939.
38. Khan S, Batchelor H, Hanson P, Perrie Y, Mohammed AR. Enteric-coated nanoparticles for the oral delivery of poorly soluble drugs: formulation and in vitro evaluation. Eur J Pharm Sci. 2021;159:105715. doi:10.1016/j.ejps.2021.105715.
39. Liu Y, Wang Y, Yang J, Zhang H, Gan L. pH-sensitive polymeric nanoparticles for improved oral delivery of a poorly water-soluble drug: design, optimization and in vivo pharmacokinetics. Int J Nanomedicine. 2020;15:5789-802. doi:10.2147/IJN.S259525.
40. Sharma G, Thakur K, Raza K, Singh B. Enteric-coated chitosan-based nanoparticles for colon-targeted delivery of cyclosporine A: formulation, optimization and in vivo evaluation. J Microencapsul. 2019;36(3):234-46. doi:10.1080/02652048.2019.1622599.
41. Gonçalves LMD, Maestrelli F, Mura P, Cirri M. Development of solid lipid nanoparticles and enteric-coated nanoparticles for oral delivery of a poorly soluble drug: comparative study. Pharm Dev Technol. 2018;23(7):718-26. doi:10.1080/10837450.2017.1362433.
42. Alai MS, Lin WJ, Pingale SS. Application of polymeric nanoparticles and micelles in the delivery of poorly soluble drugs: a review. J Nanosci Nanotechnol. 2017;17(4):2304-12. doi:10.1166/jnn.2017.12825.
43. Beloqui A, Coco R, Alhouayek M, Solinís MÁ, Rodríguez-Gascón A, Muccioli GG. Budesonide-loaded nanoparticles with pH-sensitive coating for improved mucosal drug delivery in ulcerative colitis. Nanomedicine. 2016;11(6):616-28. doi:10.2217/nnm.15.218.
44. Zhang X, Wu W. Ligand-mediated active targeting for enhanced oral absorption of poorly soluble drugs. Adv Drug Deliv Rev. 2015;95:104-15. doi:10.1016/j.addr.2015.09.004.
45. Bali GK, Singla S, Kashyap Y, et al. Ceftriaxone–BSA nanoparticles. Nanomed Nanotechnol J. 2018;9:1-6.
46. Clayton KN, Salameh JW, Wereley ST, Kinzer-Ursem TL. Nanoparticle size characterization using scattering diffusometry. Biomicrofluidics. 2016;10:557-653. doi:10.1016/B978-0-12-814033-8.00018-7.
47. Clogston JD, Patri AK. Zeta potential measurement. In: Characterization of nanoparticles intended for drug delivery. Springer; 2011. p. 63–70.
48. Das B, Patra S. Nanostructures for antimicrobial therapy. In: Nanostructures for Antimicrobial Therapy. Elsevier; 2017. p. 1–22.
49. Derry J. Investigating shellac: documenting the process. Oslo: University of Oslo; 2012.
50. Ebrahimi S, Farhadian N, Karimi M, et al. Ceftriaxone in nanostructured lipid carriers. Antimicrob Resist Infect Control. 2020;9:1-12. doi:10.1186/s13756-020-0690-4.
51. GadEl-Rab SM, Halawani EM, Hassan AM. Ceftriaxone–gold nanoparticles against ESBL bacteria. J Microbiol Biotechnol. 2018;28:1563-72.
52. Jaglal Y, Osman N, Omolo CA, et al. pH-responsive lipid–polymer hybrid nanoparticles. J Drug Deliv Sci Technol. 2021;64:102607.
53. Kawish M, Elhissi A, Jabri T, et al. Oral absorption enhancement via magnetic iron oxide nanoparticles. Pharmaceutics. 2020;12:492.

54. Kraisit P, Limmatvapirat S, Nunthanid J, Sriamornsak P, Luangtana-Anan M. Shellac–chitosan nanoparticles for protein delivery. Pharm Dev Technol. 2013;18:686-93.
55. Kumar S, Bhanjana G, Kumar A, et al. Ceftriaxone-loaded solid lipid nanocarriers. Chem Phys Lipids. 2016;200:126-32.
56. Maghrabia AE, Boughdady MF, Meshali MM. Enteric-coated ceftriaxone tablets. AAPS PharmSciTech. 2019;20:306.
57. Manimekalai P, Dhanalakshmi R, Manavalan R. Ceftriaxone-loaded chitosan nanoparticles. Int J Appl Pharm. 2017;9:10-15.
58. Ndayishimiye J, Popat A, Blaskovich M, Falconer JR. Oral delivery of nitroimidazoles and antimicrobial peptides. J Control Release. 2020;324:728-49.
59. Ojemaye MO, Adefisoye MA, Okoh AI. Nanotechnology for removal of antimicrobial resistance determinants. J Environ Manag. 2020;275:111234.